Analysis of Ultrasonic Linear Motor Using the Finite Element Method and Equivalent Circuit

Jong-Seok Rho*, Hyun-Woo Joo*, Chang-Hwan Lee and Hyun-Kyo Jung***

Abstract - In this paper, a three-dimensional finite element method and construction of equivalent-circuit for a linear ultrasonic motor are presented. The validity of three-dimensional finite element routine in this paper is experimentally confirmed by analyzing impedance of a piezoelectric transducer. Using this confirmed finite element routine, impedance and vibration mode of a linear ultrasonic motor are calculated. Elliptical motion of contact point between vibrator and rail of the linear ultrasonic motor is shown for determination of contact points. By using the finite element method and analytic equations, characteristics of the linear ultrasonic motor, such as thrust force, speed, losses, powers and efficiency, are calculated. The results are confirmed by experiment. Finally, equivalent circuit parameters of the linear ultrasonic motor are obtained using the three-dimensional finite element method and analytic equations.

Keywords: equivalent circuit, finite element method, linear motor, piezoelectric, ultrasonic motor

1. Introduction

Ultrasonic motors have received much attention in response to the need for high-torque density, low-speed at high efficiency and small weight for small power applications.

In addition to rotary USM, the linear USM is also the subject of extensive interest, having a great deal of freedom in design, high-thrust force and size. Because the USM operates with great mechanical friction and needs no additional braking system, it has precise control characteristics [1-2].

Linear USM can be classified into two categories, self-moving machine and non self-moving machine. Generally, while the thrust force of the non self-moving machine is greater, the speed of the self-moving machine is higher [3-4].

As mentioned above, USM has numerous merits, prompting researchers to perform widespread study for several decades. However, precise analysis and design remain incomplete because this machine uses a very complicated dynamic mechanism, such as electromechanical coupling and mechanical friction. Because of the USM's complexity, precise analysis and design is very difficult in the case of the analytic method. Therefore, a numerically combined analytic method is necessary for more accurate analysis.

* School of Electrical Engineering and Computer Science, Seoul National University, Seoul, Korea. (zzong@elecmech.snu.ac.kr), (hwjoo74@snu.ac.kr), (hkjung@snu.ac.kr).
** Electrical Engineering and Science Research Institute, Seoul National University, Seoul, Korea. (ichkhk@snu.ac.kr).
Received: December 2, 2002 ; Accepted: November 21, 2003

Thus, in this paper, USM is analyzed by a three-dimensional finite element method, combining analytical approaches.

2. Working Principle

Fig. 1 shows the vibrator of L1-B4 mode USM. Fig. 2 shows the operating principles.

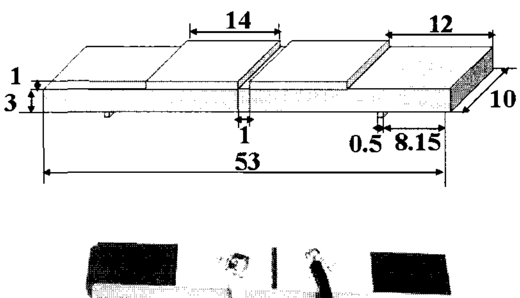

Fig. 1 - The vibrator of L1-B4 mode USM [mm]

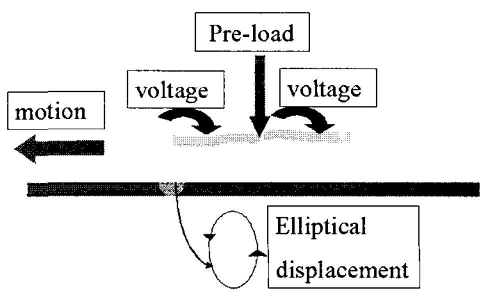

Fig. 2 The operating principle of L1-B4 mode USM

The USM operates as a result of the elliptical motion at the teeth of the vibrator. This elliptical motion is made by double-mode vibrations. Double mode vibration is composed of the first longitudinal (L1) and the fourth bending (B4). Vertical direction motion is created by bending vibration and horizontal direction motion by a longitudinal one. Fig. 3 depicts the manufactured L1-B4 mode USM.

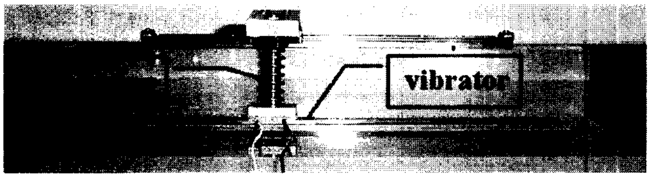

Fig. 3 L1-B4 mode USM model

3. Finite Element Formulation

The matrix equations of (1) are bases for the derivation of the finite element formulation, which relate mechanical and electrical quantities in piezoelectric media [1].

$$T = c^E S - e^t E \\ D = eS + \varepsilon^S E \quad (1)$$

T: vector of mechanical stresses
S: vector of mechanical strains
E: vector of electric field
D: vector of dielectric displacement
c^E: mechanical stiffness matrix for constant electric field E
ε^S: permittivity matrix for constant mechanical strain S
e: piezoelectric matrix; superscript t means transposed

From Hamilton's variation, the matrix equations (2) and (3) can be obtained [5].

$$-\omega^2 Mu + j\omega D_{uu} u + K_{uu} u + K_{u\Phi}\Phi = F_{total} \quad (2)$$

$$K'_{u\Phi} u + K_{\Phi\Phi}\Phi = Q_S + Q_p \quad (3)$$

K_{uu}: mechanical stiffness matrix
D_{uu} : mechanical damping matrix
$K_{u\phi}$: piezoelectric coupling matrix
$K_{\phi\phi}$: dielectric stiffness matrix
M: mass matrix
F_{total} : mechanical body forces
Q_S: electrical surface charges
Q_P: electrical point charges

4. Finite Element Results

4.1 Transducer Analysis

The electrical impedance is important since it can clearly depict the characteristic quantities such as the resonance and anti-resonance frequencies of piezoelectric devices and can be verified by simple experiments with a network analyzer. Electrical impedance can be calculated by using the external electrical charge and the potential on the electrode. Then the electrical impedance is given by (4).

$$Z(w) = \frac{\Phi(w)}{jwQ_o} \quad (4)$$

Fig. 4 indicates the impedances from three-dimensional calculations and experiments on the piezoelectric transducer test model, whose experimental impedance is referred from [1]. From these results, it is evident that the finite element analysis routine in this paper is accurate. Material data used in this paper is piezoelectric material VIBRIT 420 referred from [1].

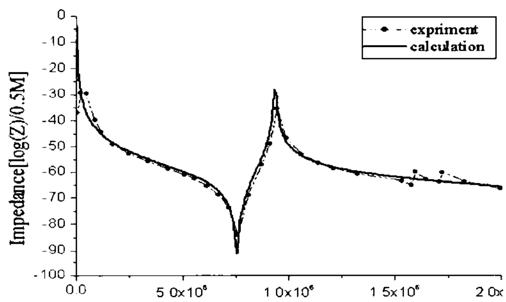

Fig. 4 Impedance of piezoelectric transducer

4.2 Analysis of Impedance

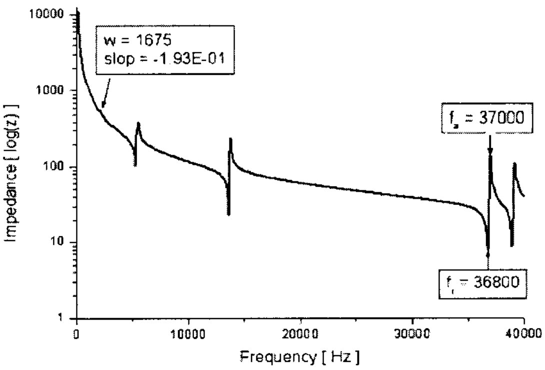

Fig. 5 Impedance of L1-B4 mode USM

Fig. 5 shows the impedance calculation of USM, taken from Fig. 1. Generally, many resonance modes exist in piezoelectric systems. However, vibration modes are different for each resonance frequency. USM in this paper is operated in suitable L1-B4 mode, with a resonance frequency of about 36.8[KHz].

4.3 Analysis of [L1-B4] Mode

Fig. 6 shows longitudinal displacement, called L1 mode. Fig. 7 illustrates vertical bending displacement, called B4 mode. From these two figures, the contact points can be determined by considering phase differences in the contact points of each mode. That means phase differences between the contact points of L1 and B4 mode should be 180 degrees for linear motion of USM.

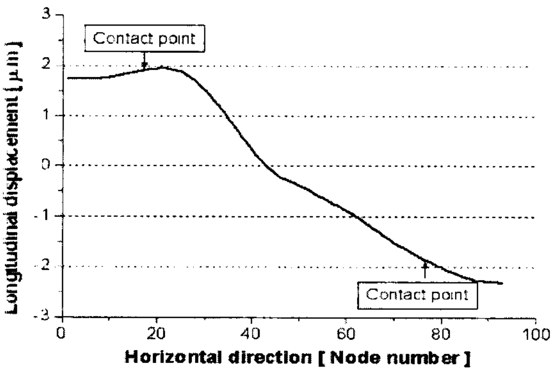

Fig. 6 L1 mode shape

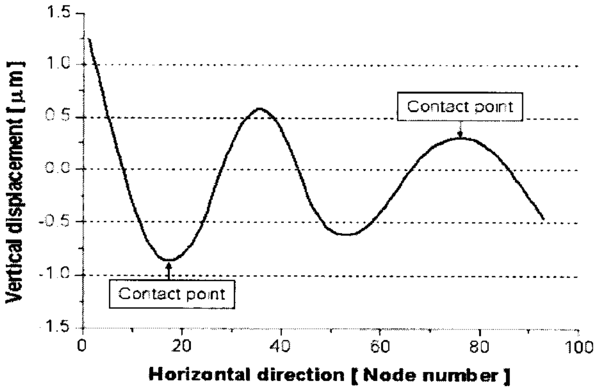

Fig. 7 B4 mode shape

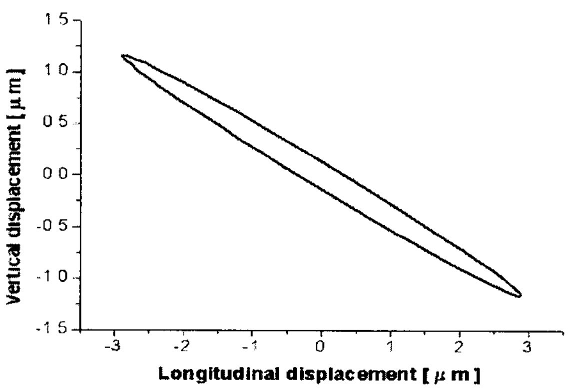

Fig. 8 Elliptical motion at the teeth point

Fig. 8 shows the elliptical motion of USM at these contact points. This motion can be derived by the combination of horizontal and vertical displacement amplitudes with the phase difference at contact points. From this result using the three-dimensional finite element method, it is verified that USM in this paper generates linear motion properly.

5. Analysis of Contact Problem

It is difficult to calculate the velocity and thrust force analytically because of complex mechanical contact problems involved in motor dynamic characteristics [3, 5]. However, using some assumptions and experimental data, a rough analytic estimation is possible.

In this paper, the deformation at contact point due to an elastic characteristic is neglected during contact period because the stress due to the preload is much higher than that of the deformation.

The displacement can be divided into two types. One type is a vertical displacement related to the thrust force. The other type is a horizontal displacement related to the speed. If there is no slip, the force is less than the normal force multiplied by a static friction coefficient. But, generally, there exists some slip, so it is assumed that the force is the same as the normal force multiplied by a dynamic friction coefficient.

Fig. 9 shows the method of mover speed calculation. When vertical displacement, related to thrust force of the vibrator is in a negative direction as shown in Fig. 8, contact between vibrator and rail occurs. In this duration, average horizontal displacement x_{ave}, related to the speed, can be calculated as shown in Fig. 8.

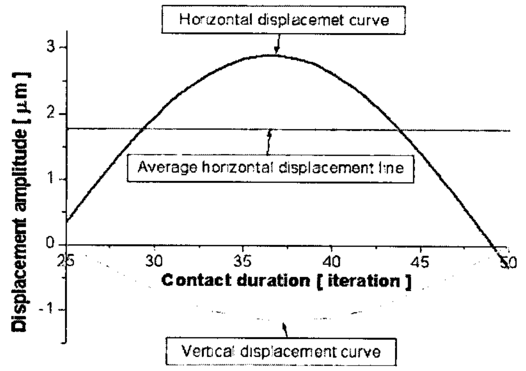

Fig. 9 Velocity decision method

As such, the average mover velocity can be calculated using equation (5).

$$V_{mov} = x_{ave} \times w \tag{5}$$

To understand and derive the contact related equations, a free-body diagram of the vibrator and rail is needed. Considering the contacting relation of vibrator and rail, the free-body diagram is drawn as illustrated in Fig. 10. That is derived in an instant, when the speed of the mover is faster than that of the vibration. So F_{fri} is determined by this speed relation, as shown in Fig. 9. In the contrary case, the speed of the mover is slower than that of the vibration and F_{fri} direction is reversed with the same strength. When stick duration occurs, vibration and mover speed are equal.

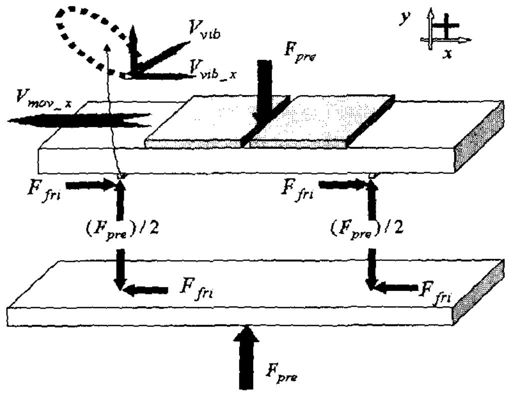

Fig. 10 Free-body diagram regarding contacting condition

V_{vib_x} can be calculated using equation (6).

$$V_{vib\_x} = x \times w \tag{6}$$

The frictional force, which occurs because of Speed difference, can be analytically formulated as in (7).

$$F_{fri} = sign[V_{mov} - V_{vib\_x}] \cdot \mu \cdot F_{pre} \tag{7}$$

$(V_{mov} - V_{vib\_x}) > 0 \rightarrow sign[V_{mov} - V_{vib\_x}] = 1$ (slip)

$(V_{mov} - V_{vib\_x}) = 0 \rightarrow sign[V_{mov} - V_{vib\_x}] = 0$ (stick)

$(V_{mov} - V_{vib\_x}) < 0 \rightarrow sign[V_{mov} - V_{vib\_x}] = -1$ (slip)

Thrust force F_{thr},

$$F_{thr} = |F_f| \tag{8}$$

Power loss due to the slip,

$$P_{slip} = |F_{fri}| \cdot |V_{mov} - V_{vib\_x}| \tag{9}$$

Output power,

$$P_{out} = F_{thr} \cdot V_{mov} \tag{10}$$

Finally, efficiency of power delivery from teeth vibration to rail is

$$\eta_{contact} = \frac{P_{out}}{P_{vibration}} = \frac{P_{out}}{P_{out} + P_{slip}} \tag{11}$$

Efficiency from input voltage to output power is

$$\eta = \frac{P_{out}}{P_{input}} \tag{12}$$

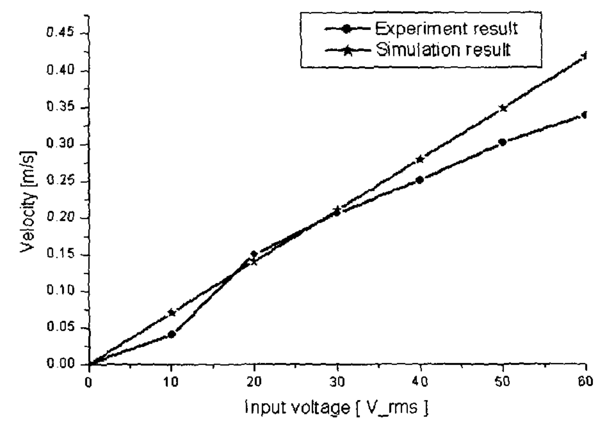

Fig. 11 Velocity of input voltage variation (preload is 0.1N)

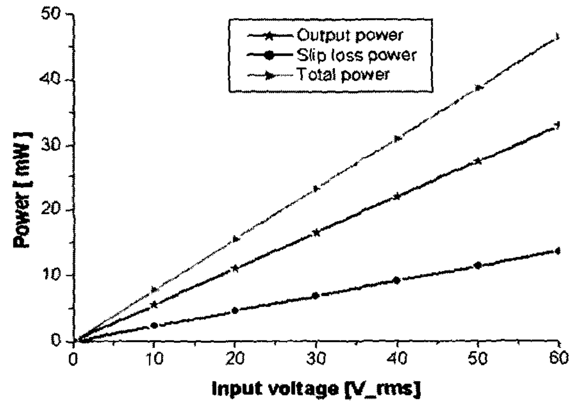

Fig. 12 Input voltage-Power relation

Table 1 Characteristics of USM (V_{in} = 60[V])

P_{in}	0.6564 [W]
V_{mov}	0.42 [m/sec]
F_{thr}	0.0785 [N]
P_{slip}	0.0135 [W]
P_{out}	0.0329 [W]
$\eta_{contact}$	70.8 [%]
η	8.51 [%]

Using these formulations, the characteristics of L1-B4 mode USM can be calculated. In this case the preload is 0.1[N], just the weight of the vibrator itself. The simulation result of velocity is confirmed by comparing the experimental result as shown in Fig. 11. And the other results are shown in Table 1 and Fig. 12.

6. Equivalent Circuit

Using the equivalent-circuit model for USM, it is simple to consider the characteristics of the motor, but this model has difficulty in finding equivalent-circuit parameters, such as capacitances, inductances, and resistance of USM, especially contact related friction resistance and load resistance. To establish equivalent-circuit for USM, equivalent-circuit parameters should be calculated numerically. Fig. 13 shows a well-accepted equivalent-circuit for a USM [3]. C_{dl} indicates capacitance due to the electrode of piezoelectric material and L and C indicates inductance and capacitance for resonance characteristics. R_{mech}, R_{slip}, and R_{out} represent the mechanical vibration loss, the loss due to slip, and the power used for moving, respectively.

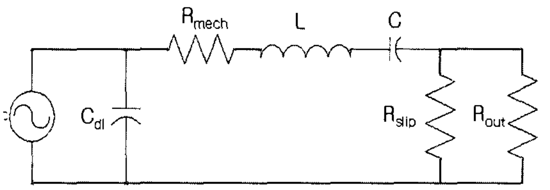

Fig. 13 Equivalent-circuit of USM

6.1 Establishment of Reactive Parameters

At first, C_{dl} parameters can be calculated by using slope at ω, as shown in Fig. 3 because the impedance of C_{dl} is dominant at a low frequency compared with resonance frequency [6].

$$C_{dl} = |1/(slope_{in} \times \omega^2)| \tag{13}$$

And next, the total input capacitance can be defined,

$$C_{Total} = C_{dl} + C \tag{14}$$

From analytic calculations of resonance and anti-resonance frequency, C_{dl} can be calculated by using (15) [4].

$$C_{dl} \cong \frac{\omega r^2}{\omega a^2} C_{Total} \tag{15}$$

Using (13) and (14) C can be calculated by using (16) [6].

$$C = C_{dl}\left(\frac{\omega a^2}{\omega r^2} - 1\right) \tag{16}$$

And from the definition of resonance frequency, inductance, L, is to be (17).

$$L = \frac{1}{\omega_r^2 C} \tag{17}$$

6.2 Establishment of Loss of USM

Losses of piezoelectric media are composed of mechanical vibration loss and dielectric loss. However, dielectric loss can be negligible because it is small compared with mechanical vibration loss [7]. Mechanical vibration loss of USM, $P_{mech\text{-}loss}$, can be computed by using finite element calculation of USM, (18) [8].

$$P_{mech-loss} = \frac{1}{2} M v^2 \omega_r Q_m^{-1} \tag{18}$$

Where, M, v, ω_r and Q_m are mass of the sample, vibrating velocity, resonant angular frequency, and mechanical quality factor, respectively. In (18), Angular frequency is obtained from Fig. 5. Vibrating velocity of USM is computed by using the angular frequency and displacements at the node, which has maximum value.

Losses due to the mechanical vibration and slip are computed by using (18) and (9). Power used for moving is calculated by using (10). The results are tabulated in Table 2.

Table 2 Vibration loss powers and loss parameters

$P_{mech-loss}$	0.0042 [W]
R_{mech}	0.1921 [Ω]
R_{slip}	0.4239 [Ω]
R_{out}	0.1739 [Ω]

7. Conclusion

In this paper, a three-dimensional finite element method and construction of equivalent-circuit for linear ultrasonic motor are presented. The validity of three-dimensional finite element routine in this paper is experimentally confirmed by analyzing impedance of a piezoelectric transducer. Using this confirmed finite element routine, impedance and vibration mode of the linear ultrasonic motor are calculated. Elliptical motion of contact point between the vibrator and rail of the linear ultrasonic motor is shown for determination of contact points. And by using the finite element method and analytic equations, characteristics of the linear ultrasonic motor, such as thrust force, speed, losses, powers and efficiency, are calculated.

In this process, the contact problem is considered. The results are confirmed by experiment results. Finally, equivalent circuit parameters of the linear ultrasonic motor are obtained by the three-dimensional finite element method and analytic equations.

There is some degree of difficulty due to the small efficiency of the L1-B4 USM, because friction is caused between the mover and rail mechanism of USM. However, because USMs have many merits, such as compact size, good breaking characteristics, silent operation, and do not require electro-magnetic fields, they can be used in many industrial applications.

References

[1] Reinhard Lerch, "Simulation of Piezoelectric Devices by Two- and Three Dimensional Finite Elements," *IEEE Transactions on Ultrasonics, Ferroelectrics and Frequency Control*, vol. 37, pp. 233-247, May 1990.

[2] Y.Jin, C.F. Foo, and W.G. Zhu, "Three Dimensional Simulation of Piezoelectric Transformer for the Switching Power Supply." *Industrial Electronics Society, 1999. IECON '99 Proceedings. The 25th Annual Conference of the IEEE*, vol. 1, pp. 295 -299, 1999.

[3] Toshiiku Sashida and Takashi Kenjo, *An Introduction to Ultrasonic Motors*, Clarendon Press, Oxford, 1993.

[4] S. Ueha, Y. Tomikawa, M. Kurosawa, and N. Nakamura, *Ultrasonic Motors: Theory and Applications*, Clarendon Press. Oxford, 1993.

[5] Hong-In Chea, *Fabrication and Characteristics Analysis of an Ultrasonic Motor using the Flexural Vibration Mode of a Ring-type Piezoelectric Ceramic*, Ph.D. Thesis, Chung-Buk National University, Korea, 1995.

[6] Chin-Yi Lin, *Design and Analysis of Piezoelectric Transformer Converter*, VPEC Ph.D. Dissertation, 1997.

[7] Yasuhiro Sasaki, Sadayuki Takahashi, and Seiji Hirose, "Relationship between Mechanical Loss and Phases of Physical Constants in Lead-Zirconate-Titanate Ceramics," *Jpn. J. Appl. Phys.* vol. 36, pp. 6058-6061, September. 1997.

[8] H. W. Katz, *Solid State Magnetic and Dielectric Devices*, John Wiley and Sons, Inc., 1959.

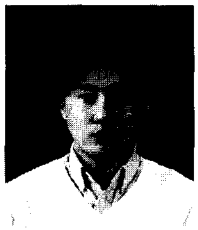

Jong-Seok Rho
He received his B.A. degree in 2001 from the School of Mechanical Engineering, Han-Yang University. His research focuses on analysis and design of piezoelectric media and numerical analysis of electrostriction fields and systems. He is currently an M.S. student at Seoul National University.

Hyun-Woo Joo
He received his B.A. degree in 2000 from the School of Electrical Engineering, Chung-Nam National University. His research focuses on analysis and design of piezoelectric media and numerical analysis of electrostriction fields and systems. He is currently a Ph.D. student at Seoul National University.

Chang-Hwan Lee
He received his B.A. degree in 1996, M.S. degree in 1998 and Ph.D. in 2002 from the School of Electrical and Computer Science Engineering, Seoul National University. His research deals with analysis and design of piezoelectric media and numerical analysis of electromagnetic fields and systems. He is now a Post Doc. at the Electrical Engineering and Science Research Institute at Seoul National University.

Hyun-Kyo Jung
He graduated from the School of Electrical and Computer Science Engineering, Seoul National University, in 1979. He received his M.S. from Seoul National University in 1981, and his Ph.D. in Electrical Engineering from Seoul National University in 1984. He worked as a faculty member at Kangwon National University from 1985 to 1994 and joined Polytechnic University in New York from 1987 to 1989. He has been teaching at the School of Electrical Engineering, Seoul National University, since 1994. From 1999 to 2000, he also served as a Visiting Professor at UC Berkley. His present interests cover various topics of the analysis and design of electric machinery and numerical field analysis of electrical systems, especially dealing with the Finite Element Method.